

TEMPERATURE DEPENDENCE OF THE ELECTRIC QUADRUPOLE INTERACTION IN PbHfO_3

Y. YESHURUN, Y. SCHLESINGER and S. HAVLIN

Department of Physics, Bar-Ilan University, Ramat-Gan, Israel

(Received 12 June 1978; accepted in revised form 8 September 1978)

Abstract—The temperature dependence of the Electric Field Gradient (EFG) in PbHfO_3 was studied in the temperature range 25–225°C by the Differential Perturbed Angular Correlation method. In the two anti-ferroelectric phases below 215°C, not too close to either transition temperature, the EFG decreases as the temperature increases toward T_c . Just above T_c an abrupt rise of EFG was observed indicating a critically behaving contribution to EFG. The results are interpreted in terms of a model based on the local static as well as time-dependent changes of the electric environment, at a lattice site. In accord with the predictions of this model the results exhibit qualitatively the P_s^2 temperature dependence of EFG far from T_c , where P_s is the sub-lattice polarization, while in close proximity to T_c the dominant contribution to EFG is due to the susceptibility χ_q connected with the soft-mode fluctuations. The derived critical exponents are in agreement with previous experimental results on related compounds and with theoretical predictions. A hitherto unobserved additional component of V_{zz} was established, behaving critically at the antiferro-paraelectric transition at 215°C. This new component is interpreted to originate in local fluctuations connected with the central mode.

1. INTRODUCTION

In a recently published article [1] we presented an analysis of a Differential Perturbed Angular Correlation (DPAC) experiment in terms of a model based on the local changes of the electric environment at a lattice site. This model relates the static as well as the time-dependent changes of the local ionic environment in (anti-) ferroelectric perovskite type crystals to the spontaneous polarization and to the susceptibility of the (sub-) lattice. The predictions of the model can be tested via the experimentally observed variation of the Electric Field Gradient (EFG) over the temperature range of interest, particularly in the immediate vicinity of the phase transition.

The potential of the EFG as a sensitive probe of the local charge distribution has been recognized for some time [2]. Forker *et al.* [3] and independently, Klyucharev *et al.* [4], were the first to demonstrate the application of the DPAC as a valuable tool for an investigation of structural phase transitions via the associated changes in EFG. However, their work on PbHfO_3 is lacking the important data in the most interesting region close enough to T_c . Examination of the results of the above two experiments reveals a similarity in their gross features. Both results exhibit clearly the existence of the three known phases of PbHfO_3 , namely the two anti-ferroelectric phases of tetragonal structure below 165°C and between 165 and 215°C, as well as the paraelectric phase, having cubic symmetry, above 215°C. In the low temperature phase both found a gradual decrease of EFG with increasing temperature and an abrupt change of EFG at 165°C. In the intermediate phase an essentially constant value of EFG was observed. Above 215°C, in the paraelectric phase, a small but finite value of EFG was established, apparently independent of temperature. However, two substantial differences between their

results are noticeable. Firstly, Forker *et al.* report a moderate decrease of EFG to a value of ~300 MHz in the low phase and then a discontinuous decrease to 240 MHz just above this temperature. This behaviour is qualitatively consistent with their static lattice-sum calculation based on the known temperature dependence of the lattice parameters. On the other hand, Klyucharev *et al.* observed a decrease of EFG to ~170 MHz below 165°C followed by an upward jump to ~210 MHz above T_c . Such behaviour cannot be accounted for by the change of the unit-cell volume, but indicates a critical behaviour of EFG near T_c . Secondly, Forker *et al.* observed a significant increase in the perturbation frequency spread δ , in the intermediate phase, which they attributed to an increased density of structural imperfections in the intermediate phase. On the other hand Klyucharev *et al.* found a constant δ over the temperature range -196°C up to 215°C, namely in both tetragonal phases.

In the present work we investigate the temperature dependence of EFG in PbHfO_3 throughout its three phases, with particular emphasis on the study of its critical behaviour in the close proximity of both transition temperatures. To achieve this goal a highly stabilized furnace and temperature control system were developed, providing a long term stability of better than 0.01°C. This made it possible to fill in the gaps of experimental information, especially in the most important regimes close to T_c , and also to resolve the apparent inconsistencies in the previous works. We found that the present results confirm the predictions of our theory [1] and exhibit clearly the critical character of the EFG near the transition temperature.

The experimental details are described in the next section. Then follows a brief presentation of the necessary theoretical background. The experimental results

and a discussion eventually conclude this communication.

2. EXPERIMENTAL

(a) Source preparation

The PbHfO_3 sample was prepared by sintering the mixture of pressed equimolar portions of PbO and HfO_2 .

About 15 mg of the polycrystalline PbHfO_3 were neutron irradiated at the SOREQ Nuclear Research Center reactor. The sample was enclosed in a thin-walled quartz-glass ampula. The activity of the source (obtained through the reaction $^{180}\text{Hf}(n, \gamma) ^{181}\text{Hf}$) at the beginning of the measurements, was $\sim 15 \mu\text{Ci}$. To reduce the dislocations caused by radiation damage, the source was annealed in an inert atmosphere for 24 hr at $\sim 700^\circ\text{C}$ and slowly cooled to room temperature, prior to the measurements. The effect of annealing was checked by observing the reduction of δ (the width of the frequency distribution, explained in paragraph *d* of present section) at room temperature.

(b) The constant temperature furnace

The sample was positioned within the sample holder of the highly temperature stabilized furnace developed and constructed according to the specific requirements of this experiment. The two principal characteristics of this system are a stability of better than 0.01°C during prolonged measuring periods typical for a PAC experiment (24–30 hr) and highly homogeneous temperature throughout the sample (estimated temperature gradient $\approx 0.001^\circ\text{C}$). The sample temperature was continuously monitored by a Miniprobe type thermistor adjacent to the sample within an isothermal silicon-grease bath. The details of the furnace and the associated electronic control and measuring system will be described elsewhere.

(c) The coincidence system

The 1.5×0.25 in. $\text{NaI}(\text{Tl})$ detector and a 1.5×1.0 in. Naton-136 plastic detector, adjusted to respond to the 133 KeV and 480 KeV γ -rays of the ^{181}Hf cascade respectively, were connected in an essentially conventional slow-fast arrangement as described in Ref. [5]. The time resolution τ of the system was 1.1–1.4 nsec FWHM.

(d) Theory of the perturbed angular correlation

The theory of the Perturbed Angular Correlation is well documented and details can be found in the literature [6]. A concise resume follows.

The angular correlation between two successive γ -rays emitted by a nucleus, in the absence of any extranuclear perturbation, is expressed as:

$$w(\theta) = 1 + A_2 P_2(\cos \theta) \quad (1)$$

where A_2 is a constant defined by the spins of the particular nucleus, $P_2(\cos \theta)$ is the regular Legendre polynomial and θ is the angle between the directions of emission of the two photons.

An interaction between the electric quadrupole moment of the nucleus and a static electric field gradient

EFG at the site of the nucleus causes a precession of the nuclear spin about the direction of EFG which results in a time-modulation of the angular correlation pattern. For a polycrystalline sample this effect can be expressed by modifying eqn (1) in the following way

$$w(\theta, t) = 1 + A_2 G_{22}(t) P_2(\cos \theta). \quad (2)$$

The perturbation factor $G_{22}(t)$ is given by the expression

$$G_{22}(t) = \sum_{n=0}^3 \sigma_n \cos \omega_n t \quad (3)$$

where ω_n are related to the quadrupole splitting of the intermediate nuclear level and σ_n are functions of the ratios of the ω_n . The ω_n themselves are proportional, for an axially symmetric EFG, to the precession frequency ω_Q given by

$$\omega_Q = \frac{eQV_{zz}}{4I(2I-1)\hbar} \quad (4)$$

where Q is the electric quadrupole moment of the nucleus, I the spin of the intermediate nuclear level and V_{zz} is the largest component of the diagonal EFG tensor.

Averaging the G_{22} given by eqn (3) over the distribution of V_{zz} due to strains and imperfections in the sample and taking into account the finite time resolution τ of the coincidence system, the experimentally observed perturbation factor G_{22} is given by [7]

$$\langle G_{22}(t) \rangle = \sum_{n=0}^3 \sigma_n \cos \omega_n t \times \exp(-\frac{1}{2} \omega_n^2 \delta^2 \tau^2) \times \exp(-\frac{1}{2} \omega_n^2 \delta^2 t^2) \quad (5)$$

where $\delta = \Delta\omega/\omega$ is the relative spread of the frequency distribution.

3. RESULTS

The coincidence time-spectra of the 133–480 KeV cascade of ^{181}Hf were accumulated at 90 and 180° angles at each temperature. To obtain practically reasonable statistics, each measurement was performed for about 30 hr. Thus, in view of the 43 day half-life of the ^{181}Hf about 20–30 temperature points were taken with each sample. The perturbation factor $A_2 G_{22}(t)$ was then obtained from the normalized time spectra $N_{180^\circ}(t)$ and $N_{90^\circ}(t)$ (after subtraction of background)

$$A_2 G_{22}(t) = 2 \frac{N_{180^\circ}(t) - N_{90^\circ}(t)}{N_{180^\circ}(t) + 2N_{90^\circ}(t)} \quad (7)$$

Typical examples of $A_2 G_{22}$ at different temperatures are shown in Fig. 1. To emphasize the change in frequency rather than the change in anisotropy note that the vertical scales are arbitrary. The experimental $A_2 G_{22}$ was fitted, using the non-linear least squares method, by the function given by eqn (5). To eliminate the effect of the spurious prompt coincidence peak the fit was carried out starting at ~ 2 nsec after $t = 0$. The values of ω_Q , δ and the asymmetry parameter $\eta = (V_{yy} - V_{xx})/V_{zz}$ at each

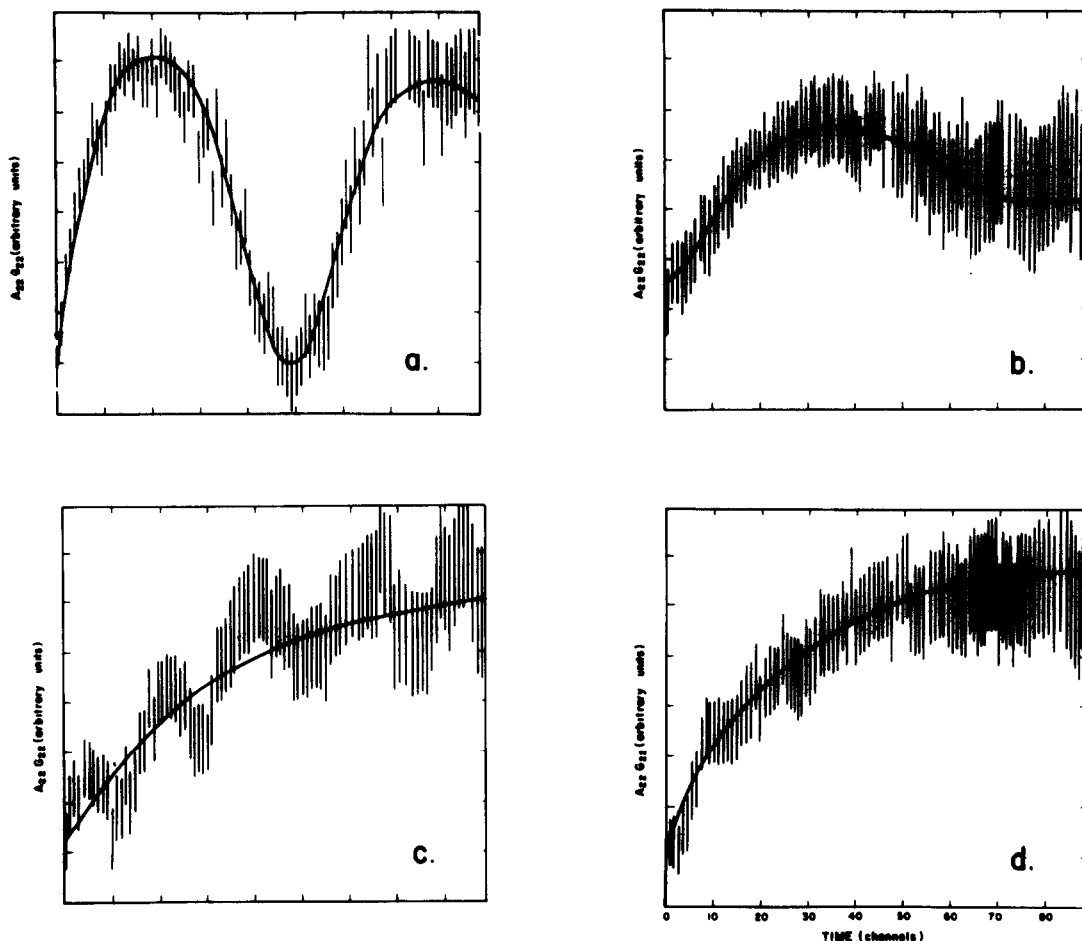


Fig. 1. Typical examples of A_2G_{22} at different temperatures: (a). 25°C, (b). 143°C, (c). 217°C and (d). 225°C. Time scale in all figures is 186 psec/channel. Channel 0 corresponds to ~ 2 nsec. The vertical scale is arbitrary and does not reflect the magnitude of the anisotropy.

temperature were deduced from the fit. The temperature dependence of ω_Q and of the relative frequency spread δ are shown in Figs. 2 and 3 respectively.

In the low temperature phase (below 165°C) ω_Q gradually decreases from about 45 MHz at room temperature to about 12 MHz just below the transition temperature. The asymmetry parameter η is apparently constant, with a value of 0.9 ± 0.1 , close to T_c . The relative frequency spread δ is $\sim 10\%$ up to 150°C then increases towards T_c (see Fig. 3).

In the intermediate phase (165–215°C) ω_Q starts with an abrupt upward jump to ~ 35 MHz just above 165°C, rapidly decreasing (within about 3°C) to 20 MHz and then decreasing gradually toward 215°C to about 4 MHz. The asymmetry parameter η is evidently constant throughout this phase with a value of 0.7 ± 0.2 . On the other hand, δ is about 15% over most of the central portion of this temperature region, but rapidly increases to $\sim 45\%$ near both transition temperatures. The present results for the behaviour of ω_Q and δ , except for the sharp rise of δ near the transition temperature, seem to be in good agreement with Klyucharev's [4] results. In the high temperature cubic phase (above $T_2 = 215^\circ\text{C}$) the analysis of the data clearly reveals an increase of ω_Q

when the temperature approaches the critical temperature T_2 (see Fig. 2). The relative frequency spread δ increases also as T approaches T_2 .

A most interesting effect was observed in the close vicinity of T_2 . Within a temperature interval of $|T - T_2| < 5^\circ\text{C}$ a small-amplitude structure of high frequency ω_H was definitely established (Fig. 1c). This high frequency component is superposed upon the main, low frequency time spectrum A_2G_{22} . The frequency of this component is strongly temperature dependent and rises sharply (within the $\pm 5^\circ\text{C}$ temperature interval about T_2) from a value of about 400 Mrad/sec to about 1500 Mrad/sec upon approaching T_2 from both sides, as shown in Fig. 4. The fact that the high frequency structure, characterized by its frequency ω_H , appears to be linearly superposed upon the main, low frequency (ω_Q) pattern, indicates the presence of two different types of sites in the crystal. The relative amplitudes of the two components represent the abundances of the corresponding sites. This permits an estimate of the abundance of the high frequency site obtaining a value of 1–3%.

A characteristic feature of the critical fluctuations within a region of $\Delta T \approx 1^\circ\text{C}$ of both transition tempera-

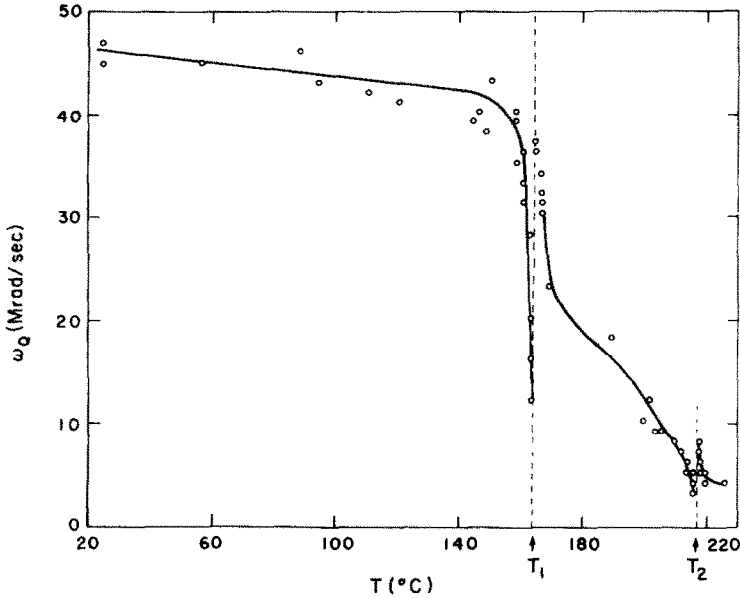


Fig. 2. Temperature dependence of the quadrupole interaction frequency ω_Q .

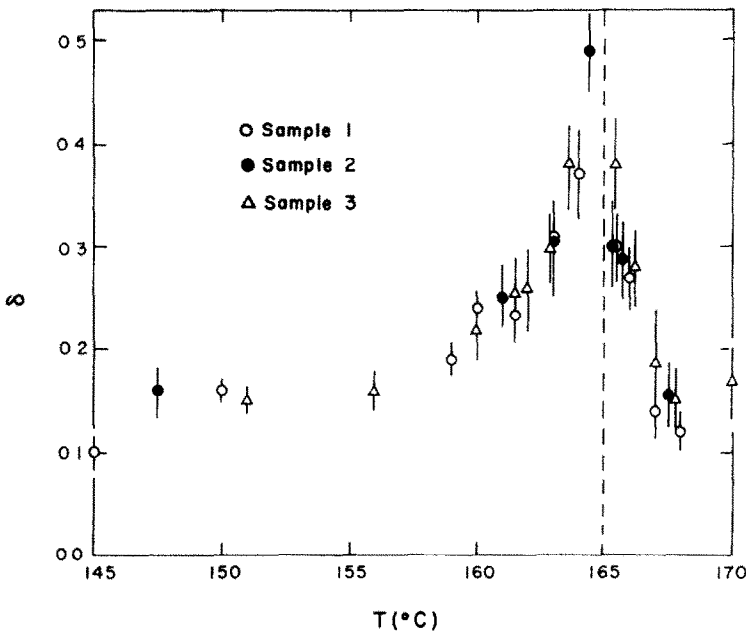


Fig. 3. Temperature dependence of the relative width δ of the distribution of the frequencies ω_Q near the AFE-AFE transition temperature.

tures is an unusual increase in the spread of the data points, preventing the derivation of reliable values of ω_Q , η and δ in this region.

4. DISCUSSION

In a recently published article [1] we presented a theoretical analysis of the temperature behaviour of V_{zz} in perovskite-type crystals as measured in a DPAC experiment. This analysis results in an expression for the experimentally determined V_{zz}^{exp} which was shown to be composed of two parts. The first part was shown to originate from the static displacements of the ions causing a distortion of the cubic phase, thus being connected

with the local polarization. The second part was shown to originate from the fluctuations of the ions about their equilibrium positions, thus being connected with the local susceptibility. These conclusions are summarized by the explicit expression

$$V_{zz}^{exp} = aP^2 + bT \sum_q \chi_q \tag{8}$$

where P_s is the (sub-) lattice spontaneous polarization of the (anti-) ferroelectric crystal and χ_q is the susceptibility connected with a wave-vector q .

Let us apply the conclusions of this theory to the case

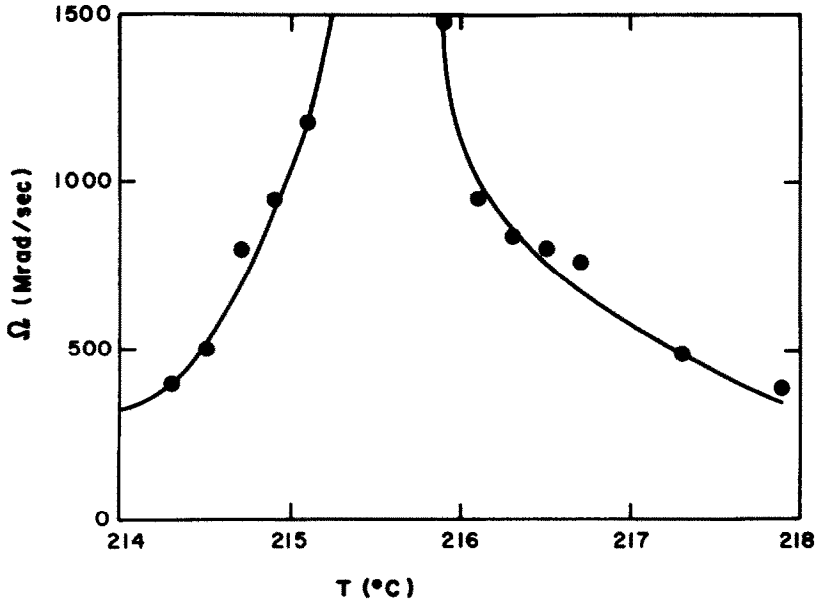


Fig. 4. Temperature dependence of the high frequency compound (HFC) near the PE phase transition.

of an anti-ferroelectric crystal (like PbHfO_3 in the present experiment). According to the theory, far below T_c the dominant contribution to V_{zz}^{exp} is given by the P_z^2 term. On approaching T_c the behaviour of V_{zz}^{exp} will be dominated by the largest term in the sum $\sum \chi_q$, namely the sublattice susceptibility χ_{qB} corresponding to the Brillouin-zone boundary wave-vector q_B . This is justified by the following arguments. Firstly, the critical behaviour of χ_{qB} near T_c is connected with the soft-mode fluctuations $\chi_{qB} \propto \omega_0^{-2}$ where ω_0 is the frequency of the soft-mode. Secondly, the enhanced contribution of χ_{qB} near T_c is connected with the q^2 behaviour of the phonon density, attaining its maximum value at the Brillouin-zone boundary.

The interpretation of the present experimental results is discussed here within the framework of this theory. It is convenient to divide this discussion into two parts: the first part deals with the region where the dominant contribution to V_{zz}^{exp} is due to the P_z^2 term in eqn (8), the second part considers the region where the fluctuations, χ_q are dominant.

The temperature dependence of $\omega_Q \propto V_{zz}^{\text{exp}}$ (see Fig. 2) below T_c is expected to follow that of P_z^2 . Such behaviour was confirmed by Bhide[8] on BaTiO_3 below T_c by a direct comparison between the independently measured P_z^2 and V_{zz} . The generally accepted form for the temperature dependence of P_z , $P_z \propto (T_c - T)^\beta$, motivates the choice of $V_{zz}^{\text{exp}} \propto (T_c - T)^{2\beta}$ as the fitting function to our data, below both T_1 and T_2 . Over most of the low-temperature phase from R.T. up to $\sim 160^\circ\text{C}$ (which is about 5°C below T_1) V_{zz}^{exp} decreases with increasing temperature in an essentially linear way confirming the molecular field result $\beta = 0.5$. Within the 5°C interval below T_1 , ($\epsilon = (T_c - T)/T_c \leq 10^{-2}$), the slope of V_{zz}^{exp} changes drastically (see Fig. 5), the critical exponent β attaining a value of 0.24 ± 0.07 and the fitted value of the critical temperature yielding $T_{c1} =$

$164.4 \pm 0.3^\circ\text{C}$. Extensive treatment on the subject of critical exponents can be found in literature[9]. Results for β similar to ours were obtained in an EPR experiment by Müller *et al.*[10] for LaAlO_3 , for SrTiO_3 . They report a value of $\beta = 0.5$ for most of the temperature region below T_c , while within $\epsilon \leq 0.1$ the value of β changed to $\sim 1/3$. This result is also in accord with the predictions of a 3-dimensional Ising model[11, 12]. The NMR experiment data of Borsa[13] in LaAlO_3 yield similar results for β .

In the corresponding 5°C interval (Fig. 6) below T_2 we obtained the values $\beta = 0.16 \pm 0.04$ and $T_{c2} = 215.5 \pm 0.3^\circ\text{C}$. The possibility of obtaining such a small value for β was already indicated by theoretical arguments[11] as well as by the results of Birgeneau *et al.*[14] on K_2NiF_4 where a value of $\beta = 0.14$ was obtained, and also by Singh and Basu[15] on KDP with $\beta = 0.16$.

Forker *et al.*[3] have shown that the results below T_c can be qualitatively accounted for by a static lattice-sum calculation. However, such calculation cannot explain the new critical phenomena near T_c observed in the present experiment.

The critical behaviour of V_{zz}^{exp} above both transition temperatures is clearly exhibited in Fig. 2. The sharp rise of V_{zz}^{exp} near both critical temperatures is in accord with the predicted dominant contribution of χ_q in the proximity of T_c as given by eqn (8). A linear fit of $[V_{zz}^{\text{exp}}(T)]^{-1} \propto (T - T_0)$ yields $T_0 = 210 \pm 1^\circ\text{C}$ which is about 5°C below T_2 . Measurements of the temperature variation of the dielectric constant of PbHfO_3 reported by Samara[16] indicate a Curie temperature $T_{0f} \approx 125^\circ\text{C}$. As Samara points out, T_{0f} is the Curie temperature of the Brillouin-zone center ($q = 0$) ferro-electric soft-mode. According to Cochran's[17] model of the phase transition in PbHfO_3 , the transition is induced by an instability of the anti-ferroelectric, Brillouin-zone boundary soft-mode, with a Curie temperature T_{0a} which

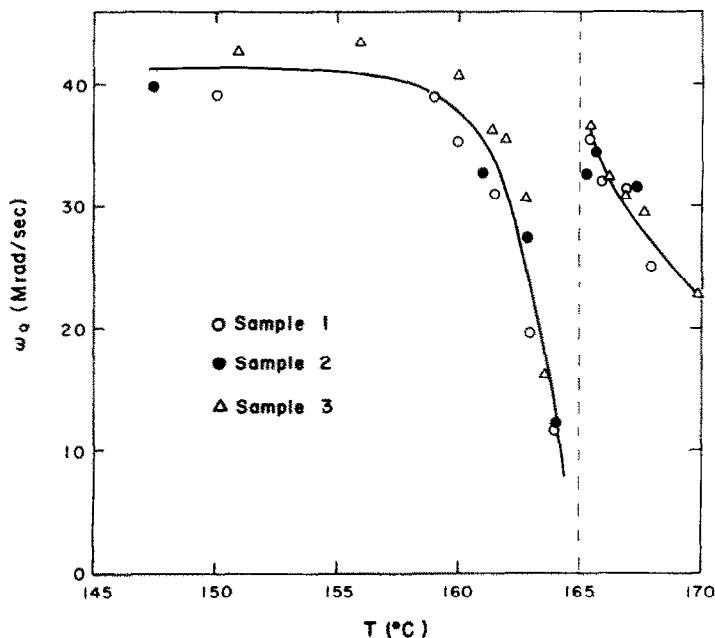


Fig. 5. Expanded portion of the ω_Q vs temperature data near the AFE-AFE transition temperature.

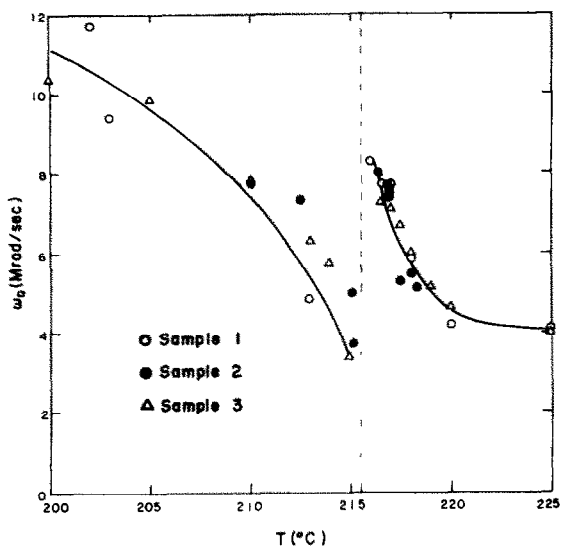


Fig. 6. Expanded portion of the ω_Q vs temperature data near the PE transition temperature.

satisfies the relation $T_{of} < T_{0a} < T_c$. The present result, exhibiting the existence of such a soft-mode with $T_0 \approx 210^\circ\text{C}$ interpreted as T_{0a} , is in agreement with the predictions of Cochran's model.

A similar linear fit of $[V_{zz}^{exp}(T)]^{-1}$ vs $T - T_0$ above the lower temperature phase transition at T_1 , yields a value of $T_0 = 117 \pm 1^\circ\text{C}$.

The superposition of the high frequency component (HFC) upon the main time-spectrum, A_2G_{22} (see Fig. 1c) was interpreted in the previous section as arising from two different types of sites in the lattice. The critical behaviour of the main component (of the lower frequency ω_Q) was dealt with above and attributed to the

soft-mode fluctuations affecting equally all probe sites in the lattice. The HFC is characterized by a relatively small abundance of the corresponding sites, by a rather high value of its frequency (which is more than about an order of magnitude larger than ω_Q) and by a strong temperature dependence near T_c (see Fig. 4). This new phenomenon cannot be accounted for by the soft-mode fluctuations, since both its additive superposition nature and small abundance indicate that this effect is of a localized character. We propose here a possible explanation for the origin of this effect. Pursuing further the ideas underlying eqn (8) we attribute this effect to an additional kind of susceptibility arising from a different behaviour of a small fraction of localized regions in the host lattice. This high susceptibility is caused by local fluctuations which are usually considered as the origin of the central mode [18, 19]. The coexistence of the soft and a central mode is well established experimentally in some perovskite compounds like SrTiO_3 and others. The intensity of the central peak rises strongly like $(T - T_c)^{-1}$, becoming dominant on approaching T_c . A commonly accepted approach for the interpretation of the central peak attributes its existence to a small concentration of defects or impurities which are more susceptible than the host [18, 20]. We attribute the high frequency component of V_{zz}^{exp} to the susceptibility caused by the local fluctuations connected with the central mode. Such description is capable of accounting for the main characteristics of HFC. The small concentration of defects explains the small abundance of the high V_{zz} sites; the rather high interaction frequency is explained by the strong intensity of the central mode near T_c and the observed temperature variation of HFC $\propto (T - T_c)^{-1}$ (see Fig. 7) is in agreement with the temperature dependence of the central peak intensity.

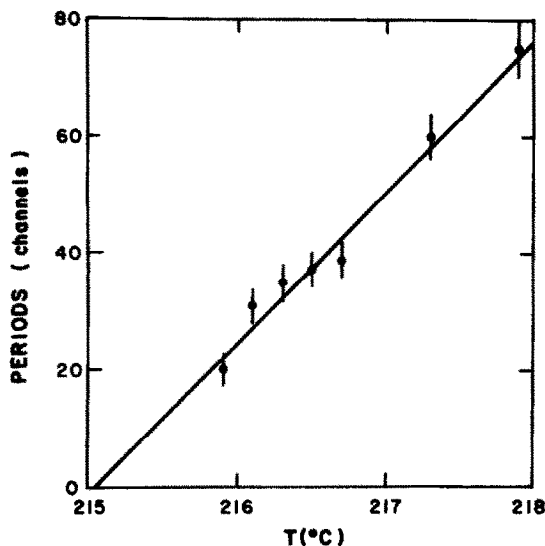


Fig. 7. Linear fit of the period $2\pi/\omega_H$ of the HFC in the PE phase.

The increase of the width δ in the vicinity of T_c is probably connected with the strong local fluctuations in the critical region, however a better understanding of this effect requires further investigations.

Acknowledgements—The authors wish to express their gratitude to Dr. P. Gluck for a critical reading of the manuscript and to Mrs. A. Oberman for the careful typing of the text. We wish to thank Mr. H. Shacham for the preparation of the samples. One of the (Y.Y.) expresses his gratitude to Dr. B. Arad and Dr. H. Zmora for their help in the first stage of this work.

REFERENCES

1. Yeshurun Y., Havlin S. and Schlesinger Y., *Solid State Commun.* **27**, 181 (1978).
2. Das T. P. and Hahn E. L., *Solid State Phys. Suppl.* **1**, 1 (1958).
3. Forker M., Hammesfahr A., Lopez-Garcia A. and Wolbeck B., *Phys. Rev.* **B7**, 1039 (1973).
4. Klyucharev V. A., Bozhko V. P., Zakurkin V. V. and Gaidamaka A. P., *Sov. Phys. Sol. State* **15**, 409 (1973).
5. Yeshurun Y. and Arad B., *J. Phys.* **C7**, 430 (1974).
6. Frauenfelder H. and Steffen R. M., In *Alpha Beta and Gamma Ray Spectroscopy*, (Edited by K. Siegbahn). North Holland, Amsterdam (1965).
7. Beraud R., Berkes I., Daniere J., Marest G. and Rougny R., *Nucl. Inst. Methods* **69**, 41 (1969). It should be noted that this form is obtained by assuming a Gaussian-type distribution for V_{zz} . The choice of a Lorentzian-type distribution leads to a somewhat different expression, however the experiment does not permit a distinction between these two distributions, see also Ref. [3].
8. Bhide V. G. and Multani M. S., *Phys. Rev.* **139**, 1983 (1965).
9. *Structural Phase Transitions and Soft Modes*, Proceedings of NATO Advanced Study Institute (1971).
10. Müller K. A., *Structural Phase Transitions and Soft Modes*, Proceedings of NATO Advanced Study Institute, p. 85 (1971).
11. Stanley H. E., *Structural Phase Transitions and Soft Modes*, Proceedings of NATO Advanced Study Institute, p. 271 (1971).
12. Schneider T. and Stoll E., *Structural Phase Transitions and Soft Modes*, Proceedings of NATO Advanced Study Institute, p. 383 (1971).
13. Borsa F., *Structural Phase Transitions and Soft Modes*, Proceedings of NATO Advanced Study Institute, p. 371 (1971).
14. Birgeneau R. J., Skalyo J. and Shirane G., *Phys. Rev.* **B3**, 1736 (1971).
15. Singh G. P. and Basu B. K., *Phys. Letts.* **64A**, 425 (1978).
16. Samara G. A., *Phys. Rev.* **B1**, 3777 (1970).
17. Cochran W., *Advan. Phys.* **9**, 387 (1960); **10**, 401 (1961).
18. Schmidt H. and Schwabl F., *Phys. Lett.* **61**, 476 (1977).
19. Halperin B. I. and Varma C. M., *Phys. Rev.* **B14**, 4030 (1976).
20. Courtens E., *Phys. Rev. Letts.* **39**, 561 (1977).